TOPICAL REVIEW — Magnetism, magnetic materials, and interdisciplinary research

Magnetic properties and magnetocaloric effects in $NaZn_{13}$-type $La(Fe, Al)_{13}$-based compounds*

Shen Bao-Gen(沈保根)†, Hu Feng-Xia(胡凤霞), Dong Qiao-Yan(董巧燕), and Sun Ji-Rong(孙继荣)

State Key Laboratory for Magnetism, Institute of Physics, Chinese Academy of Sciences, Beijing 100190, *China*

(Received 28 November 2012)

In this article, our recent progress concerning the effects of atomic substitution, magnetic field, and temperature on the magnetic and magnetocaloric properties of the $LaFe_{13-x}Al_x$ compounds are reviewed. With an increase of the aluminum content, the compounds exhibit successively an antiferromagnetic (AFM) state, a ferromagnetic (FM) state, and a mictomagnetic state. Furthermore, the AFM coupling of $LaFe_{13-x}Al_x$ can be converted to an FM one by substituting Si for Al, Co for Fe, and magnetic rare-earth *R* for La, or introducing interstitial C or H atoms. However, low doping levels lead to FM clusters embedded in an AFM matrix, and the resultant compounds can undergo, under appropriate applied fields, first an AFM–FM and then an FM–AFM phase transition while heated, with significant magnetic relaxation in the vicinity of the transition temperature. The Curie temperature of $LaFe_{13-x}Al_x$ can be shifted to room temperature by choosing appropriate contents of Co, C, or H, and a strong magnetocaloric effect can be obtained around the transition temperature. For example, for the $LaFe_{11.5}Al_{1.5}C_{0.2}H_{1.0}$ compound, the maximal entropy change reaches 13.8 $J{\cdot}kg^{-1}{\cdot}K^{-1}$ for a field change of 0–5 T, occurring around room temperature. It is 42% higher than that of Gd, and therefore, this compound is a promising room-temperature magnetic refrigerant.

Keywords: $La(Fe,Al)_{13}$ compounds, magnetocaloric effect, magnetic entropy change, magnetic phase transition

PACS: 75.30.Sg, 75.50.Bb **DOI:** 10.1088/1674-1056/22/1/017502

1. Introduction

Refrigeration plays a very important role in various fields such as industrial and agricultural production, scientific research, aerospace, medicine, and daily life, and modern society increasingly relies on the refrigeration technology. The drawbacks of the conventional gas compression-expansion technology, which is widely used today, are its high energy consumption and its adverse effect on the environment. Therefore, exploring a new type refrigeration technology that is environment-friendly and energy-efficient has become an urgent priority. Magnetic refrigeration based on the magnetocaloric effect (MCE) of magnetic materials has attracted worldwide attention because of its important application prospects.

The history of the research of magnetic refrigeration can be traced back to the year of 1881, when the MCE was first discovered by Warburg.[1] With the development of magnetic refrigeration in recent decades, magnetic refrigeration has been widely applied in the low temperature range, and meanwhile, the research on magnetic refrigeration has been gradually promoted from the low temperature range to the high temperature range. In 1976, Brown observed a large MCE in rare earth Gd (its Curie temperature T_C is 293 K) near room temperature.[2] Since then, Gd was thought to be the sole refrigerant for magnetic refrigerators working around room temperature. The maximal magnetic entropy changes (ΔS) of Gd are only 5.0 $J{\cdot}kg^{-1}{\cdot}K^{-1}$ and 9.7 $J{\cdot}kg^{-1}{\cdot}K^{-1}$ for the field changes of 0–2 T and 0–5 T, respectively.[3] Furthermore, the phase transition temperature cannot be adjusted on demand. Many scientists around the world have devoted their attention to the exploration of new MCE materials with better performance than that of Gd, and important progresses have been obtained in recent decades. In 1997, for example, Pecharsky *et al.* at the Ames lab reported that the peak value of ΔS of the rare-earth intermetallic compound $Gd_5Si_2Ge_2$ ($T_C = 274$ K) reaches 18 $J{\cdot}kg^{-1}{\cdot}K^{-1}$ for a field change of 0–5 T.[4] In the same year, Guo *et al.* at Nanjing University reported an entropy change of 5.5 $J{\cdot}kg^{-1}{\cdot}K^{-1}$ for a field change of 0–1.5 T in the manganite $La_{0.8}Ca_{0.2}MnO_3$ ($T_C = 274$ K).[5] In 2000, Hu *et al.* at the Institute of Physics, Chinese Academy of Sciences found that the Heusler alloy $Ni_{51.5}Mn_{22.7}Ga_{25.8}$ has a large ΔS of 4.1 $J{\cdot}kg^{-1}{\cdot}K^{-1}$ for a field change of 0–0.9 T associated with the martensitic–austenitic phase transition at 197 K.[6] They also found that single crystal $Ni_{52.6}Mn_{23.1}Ga_{24.3}$ exhibits a ΔS of 18 $J{\cdot}kg^{-1}{\cdot}K^{-1}$ for a field change of 0–5 T at the transition temperature of 300 K.[7] At the end of 2001 and the beginning of 2002, Kyoto University in Japan and Amsterdam University in the Netherlands reported, respectively, $MnAs_{1-x}Sb_x$[8] and

*Project supported by the National Natural Science Foundation of China, the Key Research Program of the Chinese Academy of Sciences, the National Basic Research Program of China, and the National High Technology Research and Development Program of China.

†Corresponding author. E-mail: shenbg@aphy.iphy.ac.cn

© 2013 Chinese Physical Society and IOP Publishing Ltd

$MnFeP_xAs_{1-x}$[9] compounds that show great magnetic entropy changes in the room temperature range.

No $LaFe_{13}$ binary compound with the cubic $NaZn_{13}$-type structure exists. It is necessary to introduce Al or Si atoms in order to obtain a stable $LaFe_{13}$-based compound. In the $NaZn_{13}$-type structure, La atoms occupy the 8a crystallographic site, and Fe atoms occupy the 8b and 96i sites. Fe atoms at the two sites are denoted as Fe_I and Fe_{II}, respectively. Al or Si atoms substitute for Fe_{II} randomly. La and Fe atoms at Fe_I site form a CsCl structure. The Fe_I atom is in an icosahedron formed by twelve Fe_{II} atoms, and the Fe_{II} atom is surrounded by nine other Fe_{II} atoms and one Fe_I atom at the nearest neighbor sites.[10] Based on the analysis of the phase formation rule for the $NaZn_{13}$-type compounds, we successfully synthesized the $LaFe_{13-x}Si_x$ compounds with low Si contents, and a new category of magnetic materials with large MCE was discovered.[11,12] The structure, phase transition, magnetic properties, and MCE of the $LaFe_{13-x}Si_x$ compounds have been systematically investigated by neutron diffraction, Mössbauer spectroscopy measurements, theoretical analyses based on first-principles calculations, etc. We found that the large MCE results from a negative thermal lattice expansion and a field-induced itinerant-electron metamagnetic transition.[12–17] Substituting Co for Fe or introducing interstitial atoms C/H can effectively affect the exchange interaction between the transition elements. This makes the phase transition temperature of the compounds adjustable across a wide temperature range including the room temperature while maintaining a large MCE. The maximal entropy change of the typical $LaFe_{13}$-based compounds exceeds 12 $J\cdot kg^{-1}\cdot K^{-1}$ and 20 $J\cdot kg^{-1}\cdot K^{-1}$ for the field changes of 0–2 T and 0–5 T, respectively, occurring around the room temperature.[17–25]

$LaFe_{13-x}Al_x$ compounds with $1.04 < x < 7.02$ can be stabilized in the $NaZn_{13}$-type crystalline structure.[10,26,27] Diverse magnetic ground states are observed in this system with the variation of Al content, including: (i) a mictomagnetic state in the content range of $4.9 \leq x \leq 7.0$, (ii) a soft ferromagnetic (FM) state for $1.8 < x \leq 4.9$, and (iii) an antiferromagnetic (AFM) state for $1.0 \leq x \leq 1.8$. Due to the large Fe–Fe coordination numbers and the short Fe–Fe atom distance, the AFM ordering is weak and can be easily driven into the FM state by an external magnetic field, accompanied with a significant lattice expansion.[27,28] Further investigations revealed that other techniques can also drive the AFM–FM switching, such as adjusting the ratio between Fe and Al, replacing Fe with Co or La with Ce, Pr, or Nd, or introducing interstitial atoms C or H.[29–40] When x is located in the critical content range between the AFM and FM states, a thermal driven FM–AFM phase transition occurs. Around this transition, large MCEs that satisfy the requirements of the Ericsson-cycle refrigerator were observed.[33,41] The magnetic and magnetocaloric properties of $LaFe_{11.4}Al_{1.6-x}Si_x$, $La_{1-x}R_xFe_{13-y}Al_y$ (R=Ce, Pr, Nd), $LaFe_{13-x}Al_xZ_y$ (Z=H, C), and $LaFe_{13-x-y}T_xAl_y$ (T=Mn, Co) have also been systematically investigated. In this paper, we review our recent progresses, emphasizing the effects of Al, La, and Fe site substitution and interstitial atomic effects, and the effects of magnetic field and temperature on the phase transition, and the magnetic and magnetocaloric properties of the compounds.

2. Influences of Mn and Co substitution for Fe on magnetic properties and magnetocaloric effects of $LaFe_{13-x}Al_x$compounds

In 2000, Hu *et al.*[10,30] first reported on the magnetic properties and magnetocaloric effects of $LaFe_{13-x}Al_x$-based compounds, and found that introducing a small amount of Co can convert the AFM coupling to the FM one for the $LaFe_{13-x}Al_x$ compounds with an AFM ground state. For example, the $LaFe_{11.12}Co_{0.71}Al_{1.17}$ compound exhibits the typical FM behavior with a second-order phase transition at T_C = 279 K, and large ΔS is found around T_C. The peak values of ΔS are about 4.6 $J\cdot kg^{-1}\cdot K^{-1}$ and 9.1 $J\cdot kg^{-1}\cdot K^{-1}$ under the field changes of 0–2 T and 0–5 T, respectively,[10] which are comparable with the results of Gd (5.0 $J\cdot kg^{-1}\cdot K^{-1}$ and 9.7 $J\cdot kg^{-1}\cdot K^{-1}$, T_C = 293 K[3]). For $La(Fe_{1-x}Co_x)_{11.7}Al_{1.3}$ compounds, T_C grows monotonically with the increasing Co content. It is located at 197 K when $x = 0.02$ and increases to 309 K when $x = 0.08$. Figure 1 displays the temperature dependence of the magnetic entropy change of $La(Fe_{1-x}Co_x)_{11.7}Al_{1.3}$. Although the maximum value of the magnetic entropy change reduces slightly with the increase of Co content, it still has a considerable magnitude around room temperature. Furthermore, the proper Co-to-Al ratio can also drive the Curie temperature to room temperature while retaining a large MCE. For instance, the T_C of $LaFe_{10.88}Co_{0.95}Al_{1.17}$ is 303 K, and the peak values of ΔS are 4.5 $J\cdot kg^{-1}\cdot K^{-1}$ and 9.0 $J\cdot kg^{-1}\cdot K^{-1}$ under the field changes of 0–2 T and 0–5 T, respectively. The large ΔS originates from the high saturation magnetization and a sharp magnetization change around T_C. The average magnetic moment per magnetic atom reaches 2.1 μ_B in the $LaFe_{10.88}Co_{0.95}Al_{1.17}$ compound.[31]

The crystal structure and the magnetic properties of the $LaCo_{0.7}Fe_{12.3-x}Al_x$ ($1.5 \leq x \leq 4.68$) compounds were investigated by Wang *et al.*[42] FM behavior is observed when the content of Al is increased from 1.5 to 4.68. With the increase of Al content, the lattice parameter grows monotonously, whereas T_C first increases and then, after a maximal value (315 K) at $x = 2.6$, decreases. There are five different Fe–Fe distances between the nearest neighbor Fe atoms for the $NaZn_{13}$-type structure: one between Fe_I and Fe_{II} and the other four between Fe_{II} and Fe_{II}. The variation of the five Fe–Fe

distances and the nearest neighbor number of Fe atoms with the change of Al content determines the variation trend of T_C.

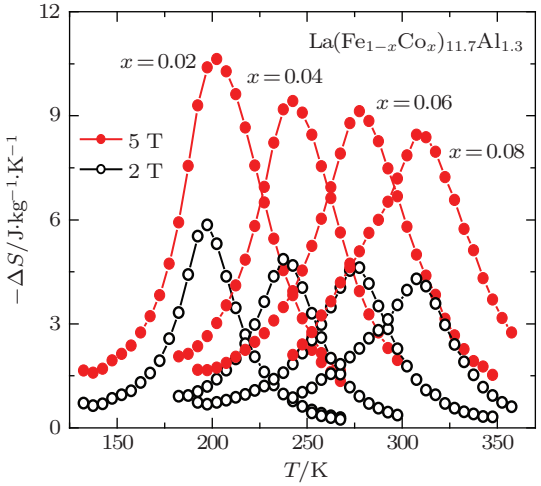


Fig. 1. Temperature dependence of the magnetic entropy change of $La(Fe_{1-x}Co_x)_{11.7}Al_{1.3}$ ($x = 0.02, 0.04, 0.06, 0.08$) compounds for magnetic field changes of 0–2 T and 0–5 T, respectively.

Wang *et al.*[43] investigated the substitution effect of Mn for Fe on the magnetic properties of $La(Fe_{1-y}Mn_y)_{11.4}Al_{1.6}$ and found that the compounds keep the $NaZn_{13}$-type structure in the content range of $0 \leq y \leq 0.25$, although the lattice constant increases linearly with the increasing content of Mn due to the larger atomic radius of Mn compared with that of Fe. Meanwhile, the magnetic properties of $LaFe_{13-x}Al_x$ show a strong dependence on the local coordination environment and the lattice volume. For samples with $y = 0.05, 0.10$, a field-induced metamagnetic transition takes place, leading to a ferromagnetic order. However, when the Mn content exceeds $y = 0.15$, the long-range magnetic order disappears. As mentioned above, the replacement of Fe by Mn slightly enlarges the lattice and therefore the Fe–Fe atomic distance. As a result, the weak AFM coupling between Fe atoms is changed to the FM coupling. Meanwhile, the AFM coupling between Fe and Mn strengthens with the increasing Mn content. The competition between the FM and the AFM couplings leads to a spin-glass behavior. It was experimentally found that the spin-glass behavior prevails in the content range of $0.05 \leq y \leq 0.25$, and increasing Mn content causes a reduction in freezing temperature.

3. Effect of substituting Si for Al on magnetic properties and magnetocaloric effects of $LaFe_{13-x}Al_x$compounds

Dong *et al.*[44] studied the effect of the replacement of Al by Si on the magnetic properties and the MCE of $LaFe_{11.4}Al_{1.6}$. They found that the lattice parameter of $LaFe_{11.4}Al_{1.6-x}Si_x$ decreases nearly linearly with the increasing Si content. Figure 2(a) presents a magnetic phase diagram of $LaFe_{11.4}Al_{1.6-x}Si_x$ ($0 \leq x \leq 1.6$). The compounds are AFM when the Si content $x \leq 0.20$. With increasing temperature an AFM-paramagnetic (PM) transition occurs at the Neel temperature T_N, which decreases with the increase of Si content. However, when the Si content is $x = 0.22$, a cusp appears in thermal magnetization curves below $T_N \sim 191$ K (Fig. 2(b)). This is the result of a regular distribution of FM clusters in the AFM background. Further increasing Si content to $0.25 \leq x \leq 0.40$ leads to an FM ordering at low temperatures. An FM–AFM transition and an AFM–PM transition appear successively upon warming. The FM–AFM transition temperature T_0 increases rapidly with Si content. With the Si content being $0.50 \leq x \leq 1.60$, the FM properties prevail, and only an FM–PM transition occurs at T_C, which increases with the increasing Si content. However, the change of saturation magnetization is rather small with the replacement of Al by Si, indicating that the Fe moment is nearly unchanged.

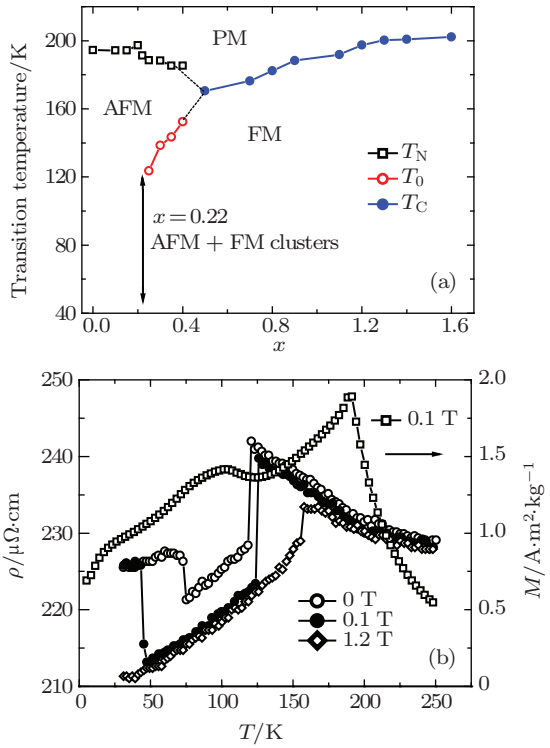


Fig. 2. (a) Magnetic phase diagram in a magnetic field of 0.1 T for $LaFe_{11.4}Al_{1.6-x}Si_x$ ($0 \leq x \leq 1.6$) compounds. The solid and the dotted lines indicate magnetic phase boundaries, T_N, T_0, and T_C indicate AFM–PM, FM–AFM, and FM–PM transition temperatures, respectively, and '↕' illustrates the temperature region where FM clusters grow from the AFM background for the compound with $x = 0.22$.[44] (b) Temperature dependence of electrical resistivity under different magnetic fields and the corresponding magnetization in a magnetic field of 0.1 T for $LaFe_{11.4}Al_{1.6-x}Si_x$ ($x = 0.22$) compound.

Figure 2(b) displays the temperature-dependent resistivity of $LaFe_{11.4}Al_{1.6-x}Si_x$ ($x = 0.22$). With the increase of temperature, the resistivity first increases, then suddenly drops at 75 K, and then linearly increases again until an abrupt jump that is followed by a monotonic decrease. When an external magnetic field is applied, the resistivity-temperature dependence is very similar to the case of $H = 0$. With the increase

of magnetic field, the critical temperature for the resistivity drop shifts to low temperatures, while the one for the resistivity jump shifts to high temperatures. This fact manifests the notable effect of magnetic field on the FM clusters and the transition temperatures. Compared with the magnetization–temperature relation, a correspondence between the two abrupt resistivity changes and the AFM–FM and FM–PM transitions can be found: the resistivity in the AFM state is biggest, while it is lowest in the FM state and intermediate in the PM state. These phenomena can be understood based on a two-fluid model.[27]

According to the phase transition characteristics, Dong *et al.*[44] chose representative compounds $LaFe_{11.4}Al_{1.6-x}Si_x$ ($x = 0.3$, 0.8) and investigated their MCE. As shown in Fig. 3, for $LaFe_{11.4}Al_{1.6-x}Si_x$ ($x = 0.3$), two entropy change peaks corresponding to the AFM–FM and FM–PM transitions appear at T_0 and T_N, respectively. The peak value at T_0 reaches 25–30 $J{\cdot}kg^{-1}{\cdot}K^{-1}$, but this is a false signal caused by the Maxwell relation.[45,46] Under a relatively high magnetic field, the two peaks merge into one table-like peak with a maximal value of 7.8 $J{\cdot}kg^{-1}{\cdot}K^{-1}$ and a temperature span of $\sim$ 70 K. For $LaFe_{11.4}Al_{1.6-x}Si_x$ ($x = 0.8$), the entropy change peaks at 182 K, corresponding to the FM–PM magnetic transition. The maximal entropy changes are 9.1 $J{\cdot}kg^{-1}{\cdot}K^{-1}$ and 14.0 $J{\cdot}kg^{-1}{\cdot}K^{-1}$ for the field changes of 0–2 T and 0–5 T, respectively. The large entropy change is caused by the specific composition, which is located at a critical point between the first-order and the second-order phase transitions.

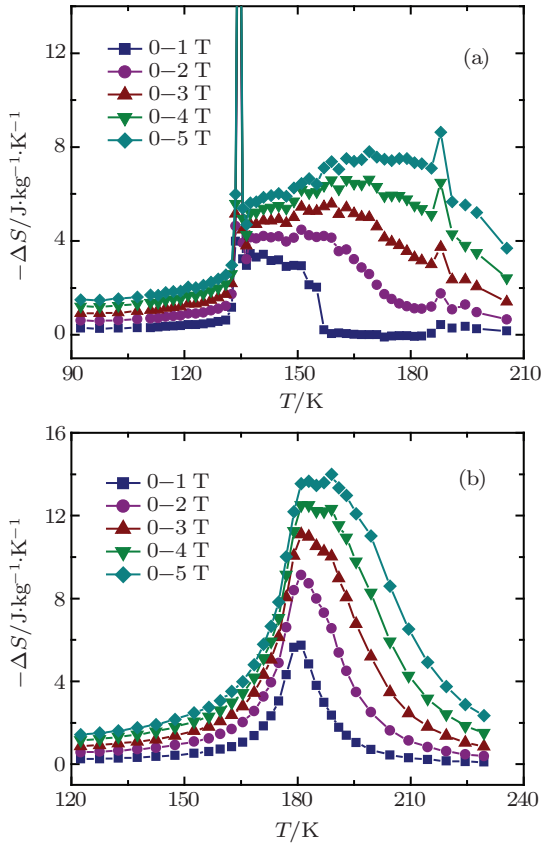


Fig. 3. Temperature dependence of the magnetic entropy change of $LaFe_{11.4}Al_{1.6-x}Si_x$ ($x = 0.3$ (a), 0.8 (b)) compounds for different magnetic field changes up to $H = 5$ T.[44]

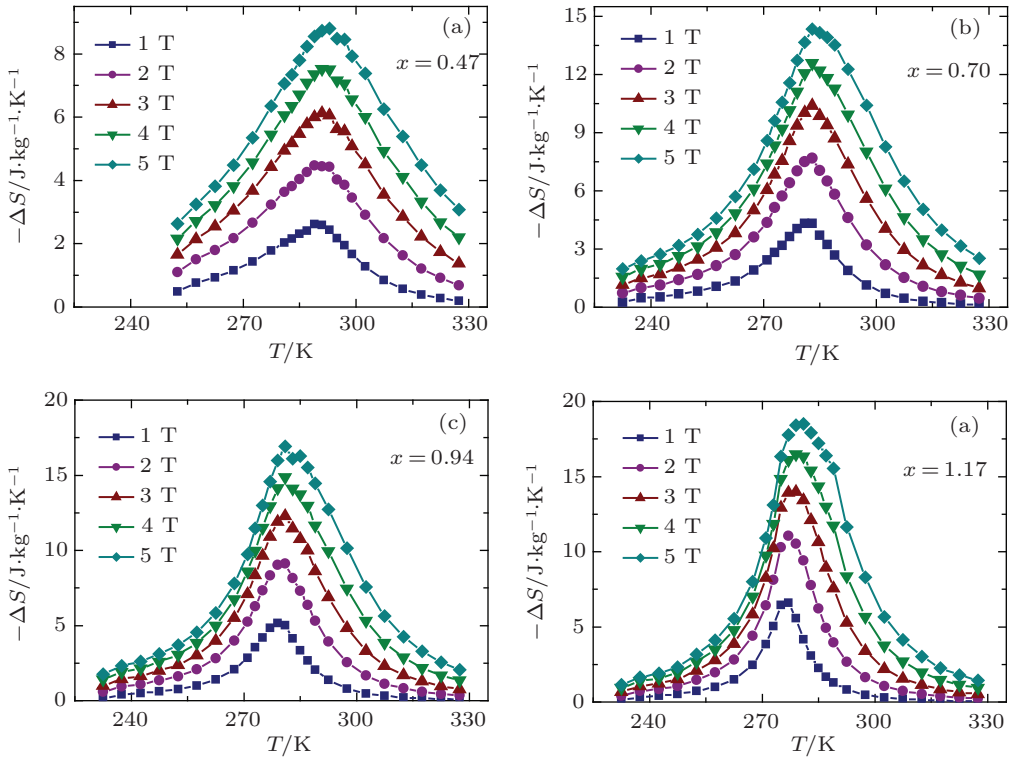


Fig. 4. Temperature dependence of the magnetic entropy change of $LaFe_{11.03}Co_{0.8}Al_{1.17-x}Si_x$ ($x = 0.47$ (a), 0.70 (b), 0.94 (c), 1.17 (d)) compounds for different magnetic field changes up to $H = 5$ T.[47]

Shen *et al.*[47] investigated magnetic and magnetocaloric properties for $LaFe_{11.03}Co_{0.8}Al_{1.17-x}Si_x$ ($0.47 < x \leq 1.17$), and found that only an FM–PM transition occurs for all compositions and T_C decreases but ΔS increases with the increasing Si content. Figure 4 presents ΔS as a function of temperature under different fields for $LaFe_{11.03}Co_{0.8}Al_{1.17-x}Si_x$. For the field changes of 0–2 T and 0–5 T, the maximal values of ΔS are, respectively, 4.5 $J{\cdot}kg^{-1}{\cdot}K^{-1}$ and 8.8 $J{\cdot}kg^{-1}{\cdot}K^{-1}$ for $x = 0.47$, and 11.0 $J{\cdot}kg^{-1}{\cdot}K^{-1}$ and 18.5 $J{\cdot}kg^{-1}{\cdot}K^{-1}$ for $x = 1.17$. The growth of ΔS is caused by the change of the transition nature from second-order to first-order, and the concurrent enlargement of lattice expansion during the magnetic transition, as well as the enhancement of the itinerant electron metamagnetic behavior.[11,16]

4. Effect of substituting magnetic rare earth *R* for La on the magnetic and magnetocaloric properties of $LaFe_{13-x}Al_x$

For the $LaFe_{13-x}Al_x$ intermetallics with an AFM ground state, the replacement of La by magnetic rare earth *R* will produce an obvious effect on the crystal structure, magnetic, and magnetocaloric properties. The work of Wang *et al.*[40,48] indicates that the substitution ratio of replacing La by light rare earth *R* generally cannot exceed 30% while keeping a stable $NaZn_{13}$-type structure. As heavy rare earth *R* is introduced to replace La, a single phase can be hardly obtained. This fact indicates that the *R* element with a large radius favors the stable $NaZn_{13}$ structure. Due to the lanthanide contraction, the replacement of La by magnetic rare earth *R* causes a lattice contraction, leading to a variation in the Fe–Fe, Fe–Al–Fe bond lengths and the Fe–Al–Fe bond angles. Meanwhile *R*–Fe and *R*–*R* interactions are introduced. The combined effect results in the weakening of the AFM behavior. As has been experimentally shown, increasing the *R* content causes a slow low temperature shift of T_N and a reduction of the critical field driving the AFM–FM transition. The latter indicates that the field-induced AFM–FM transition becomes easier as La is replaced by magnetic *R*. The substitution effect on the magnetic properties enhances along the sequence of Ce, Pr, and Nd; and the Nd doping yields the strongest effect. Figure 5 displays the magnetization curves measured at 5 K for $La_{1-x}R_xFe_{11.5}Al_{1.5}$ (*R*=Ce, Pr, Nd). The critical field to drive the AFM–FM transition is 4.1 T (3.6 T) for the Ce (Pr) substitution, and it is nearly zero for the Nd case.

Dong *et al.*[49] and Chen *et al.*[39] reported the effect of the replacement of La by Pr on magnetic properties and phase transitions for $LaFe_{11.4}Al_{1.6}$. From thermal magnetization curves measured under a low field of $H = 0.01$ T, they found that T_N is located at $\sim$ 188 K and a cusp appears below T_N, similar to the case of $LaFe_{11.4}Al_{1.6-x}Si_x$ ($x = 0.22$). This is caused by the existence of FM clusters in the AFM background. The only difference is the irregular distribution of FM clusters in the AFM background for $La_{0.8}Pr_{0.2}Fe_{11.4}Al_{1.6}$. From the temperature-dependent magnetization (*M*–*T* curve) measured under different magnetic fields, we can learn that magnetic field-driven AFM–FM and FM–AFM transitions take place. The peak at low temperature in the *M*–*T* curve becomes table-like and its height grows, indicating the increase of the FM component with the increasing magnetic field. Figure 6 shows the *M*–*T* curve measured at $H = 0.45$ T for $La_{0.8}Pr_{0.2}Fe_{11.4}Al_{1.6}$, where ZFC, FCC, and FCW refer to the modes of zero-field cooling and measuring on heating, field cooling and synchronously measuring, and field cooling and measuring on heating, respectively. The FCC and FCW curves show an obvious discrepancy around the FM–AFM transition, a typical feature of the first-order phase transition. Moreover, all the *M*–*T* curves obtained via the ZFC, FCC, and FCW modes display many discontinuous jumps and steps, manifesting the metastable characteristics of the magnetic state.

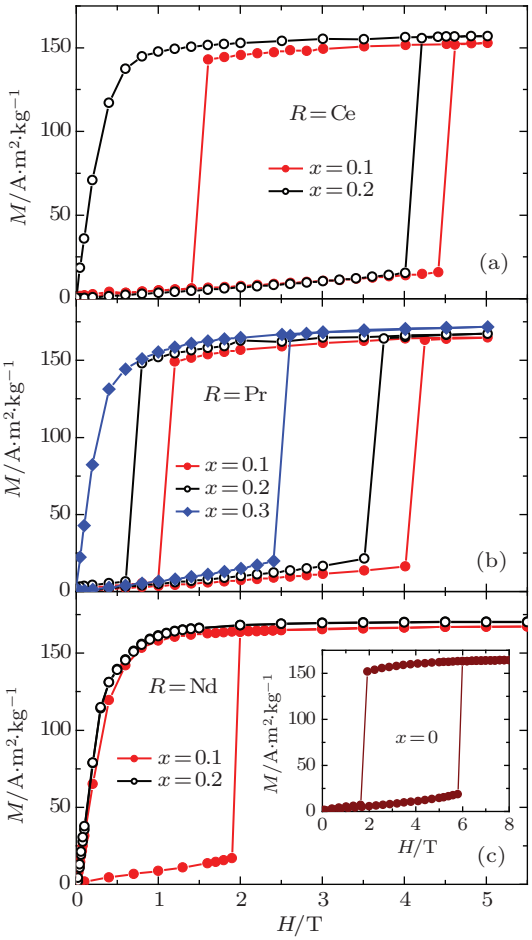


Fig. 5. Isothermal magnetization curves of $La_{1-x}R_xFe_{11.5}Al_{1.5}$ (*R*=Ce (a), Pr (b), Nd (c)) compounds at 5 K in the field-ascending and field-descending processes.[48]

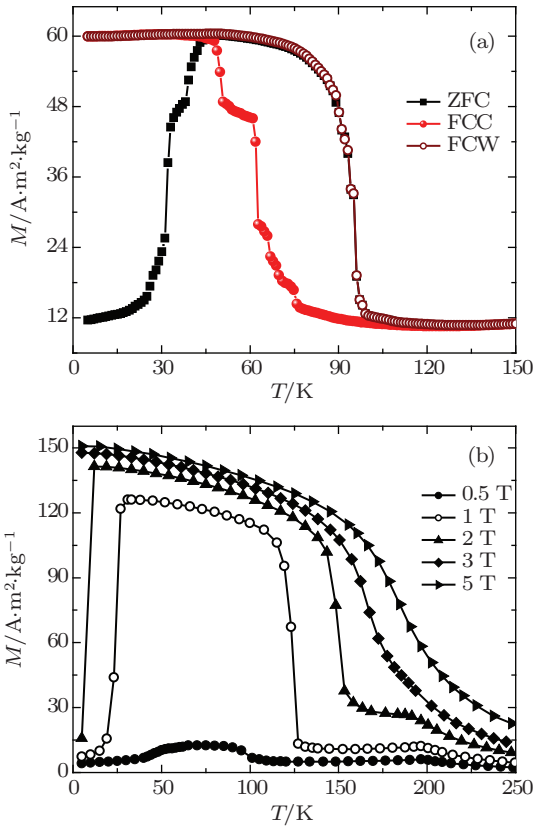


Fig. 6. (a) Temperature dependence of the magnetization for $La_{0.8}Pr_{0.2}Fe_{11.4}Al_{1.6}$ measured in ZFC, FCC, and FCW modes under a magnetic field of 0.45 T.[49] (b) Temperature dependence of the magnetization for $La_{0.9}Nd_{0.1}Fe_{11.5}Al_{1.5}$ compound under different magnetic fields.[37]

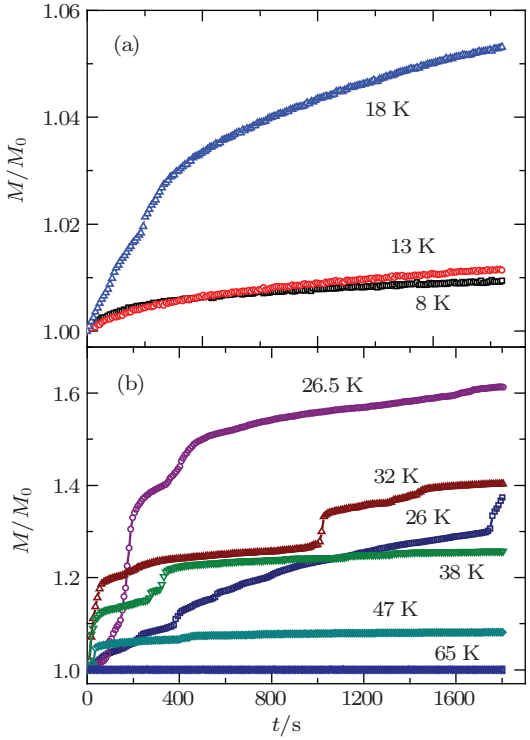


Fig. 7. Reduced magnetization M/M_0 versus time t for $La_{0.8}Pr_{0.2}Fe_{11.4}Al_{1.6}$ measured at typical temperatures under $H = 0.45$ T in the ZFC mode.[49] At each T, M_0 is the value of the magnetization recorded when the relaxation measurements were started, i.e., 0 s after the target H and T values were reached.

The magnetic metastable behavior is further studied through measuring the time-dependent magnetization at different temperatures. Figure 7 presents the reduced magnetization of $La_{0.8}Pr_{0.2}Fe_{11.4}Al_{1.6}$ as a function of time, measured under a field of 0.45 T in the ZFC mode. At temperatures below the AFM–FM transition, the magnetization is nearly unchanged with time, i.e., the system remains in the AFM state. With an increase of temperature, the relaxation behavior is obviously enhanced, and the magnetization increases significantly with time. This fact reflects the formation and growth of ferromagnetic phases. At temperatures near the AFM–FM transition point, the magnetization shows discontinuous jumps and steps, a signature of the strong competition between the AFM and the FM orderings. In the temperature range above the AFM–FM transition, however, the relaxation phenomena cannot be observed. This indicates that the AFM–FM transition is completed. For either the ZFC or the FCC mode, the magnetization–time dependence can be classified into two categories: the first one has a logarithmic, instead of exponential, relationship, which indicates a distribution of the energy barriers, and the second one is a stepwise magnetization change with time. The latter could be a signature for the nucleation and growth of magnetic phases under the applied field similar to martensite domains[50] or the inhomogeneous distribution of substituted rare earth elements in the compounds.[37]

Investigations carried out by Wang *et al.*[40] reveal that the T_N of $La_{1-x}Nd_xFe_{11.5}Al_{1.5}$ decreases from 205 K to 188 K as the Nd content increases from $x = 0$ to 0.2. When the Nd content is low, such as $x = 0.1$, the lattice distortion is small, and therefore the changes in the Fe–Fe, Fe–Al–Fe bond lengths and the Al–Fe–Al bond angles are small. Meanwhile, the number of Nd–Fe pairs with FM coupling is few. As a result, the AFM coupling prevails, and the FM clusters appear only in some local regions. With the Nd content increased to $x > 0.2$, the Nd–Fe FM pairs grow, and Fe–Fe and Fe–Al–Fe bond lengths and bond angles change significantly. The AFM coupling is destroyed, and the FM ordering prevails. Liu *et al.*[37] and Wang *et al.*[40] investigated the phase diagram of $La_{0.9}Nd_{0.1}Fe_{11.5}Al_{1.5}$ and found an obvious enhancement of the FM characteristics of the magnetic clusters with the applied field. Under a constant field below 3 T, AFM–FM, FM–AFM, and AFM–PM transitions appear successively during the warming process. A higher magnetic field causes a lower/higher temperature shift of the AFM–FM/FM–AFM transition, and a slight decrease of T_N. Further investigations indicate that a large magnetic entropy change appears around the FM–AFM transition. Wang *et al.*[40] investigated the magnetic entropy change based on both magnetic and heat capacity measurements and found that the results obtained from different techniques are consistent with each other. This fact proves that it is reasonable to use the Maxwell relations to calculate the entropy change accompanying the first-order phase

transition. For a field change of 0–5 T, the maximal ΔS is 9 J·kg^{-1}·K^{-1} for $La_{0.8}Nd_{0.2}Fe_{11.5}Al_{1.5}$, nearly the same as that of Gd. However, due to the large heat capacity of the $La(Fe_{1-x}Al_x)_{13}$-based compound, the adiabatic temperature change is only one third of that of Gd. Fortunately, the adverse effect caused by the large lattice capacity can be avoided by choosing a suitable mode of refrigeration. For example, refrigerants in refrigerators based on the Ericsson cycle are required to have nearly constant magnetocaloric values over a wide temperature range. $La_{0.8}Nd_{0.2}Fe_{11.5}Al_{1.5}$ undergoes two successive transitions at two close temperatures, which results in a nearly constant entropy change across a wide temperature range.

5. Effect of introducing interstitial C or H atoms on magnetic and magnetocaloric properties of $LaFe_{13-x}Al_x$

Wang *et al.*[34] and Chen *et al.*[51] investigated the effect of interstitial C atoms on the magnetic and magnetocaloric properties of $LaFe_{13-x}Al_xC_y$. They found that the concentration of C generally cannot exceed $y = 0.5$ and 0.8 to get a stable $NaZn_{13}$ structure for the intermetallics of $x = 1.5$ and 1.6, respectively, and the introduction of C causes a lattice expansion. It is fascinating that the introduction of a small amount of C, such as $y = 0.1$, can completely convert the AFM ordering in $LaFe_{13-x}Al_x$ into an FM ordering, and the Curie temperature increases monotonously with the increasing content of C. For example, T_C of $LaFe_{11.5}Al_{1.5}C_y$ increases from 191 K to 262 K as the C content changes from $y = 0.1$ to $y = 0.5$. A linear relation between T_C and the lattice parameter is further observed. Experiments show that the effect of interstitial atoms on T_C is two-fold. First, it narrows the 3d energy band as a consequence of the lattice expansion that reduces the overlap of the Fe 3d electron wave functions. As a result, the FM interaction is enhanced and T_C grows. Second, it produces a hybridization of the C and Fe electron orbits, and thus a decrease of T_C. The observed increase of T_C with the lattice parameter indicates that the effect of lattice expansion plays a dominant role. Besides, the saturated magnetization increases slightly with the increasing C content. The MCE of $LaFe_{11.5}Al_{1.5}C_y$ was studied by magnetic measurements,[34] and the obtained entropy change is comparable to that of Gd, as shown in Fig. 8.

To profoundly understand the effect of C introduction on the magnetic properties of the AFM $LaFe_{13-x}Al_x$ compounds, Zhang *et al.*[38] prepared $LaFe_{11.4}Al_{1.6}C_y$ ($0 < y \leq 0.08$). Investigations revealed the coexistence of the AFM and FM clusters in the compound with $y = 0.02$ and the occurrence of AFM–FM and FM–AFM transitions under external fields. These phenomena are very similar to those observed in $LaFe_{11.4}Al_{1.6-x}Si_x$ ($x = 0.22$), $La_{0.8}Pr_{0.2}Fe_{11.4}Al_{1.6}$, and $La_{0.9}Nd_{0.1}Fe_{11.5}Al_{1.5}$. Furthermore, many stepwise magnetization changes were observed around the AFM–FM and FM–AFM transitions, manifesting the metastable characteristics of the magnetic state.[52] When $y = 0.04$ or 0.06, the ground state converts from AFM to FM, and two FM–AFM and AFM–FM transitions occur successively. With the increase of C content, the FM–AFM transition shifts to high temperatures. For the compound of $y = 0.08$, the temperature of the FM–AFM transition coincides with the Neel temperature, and the compound displays a simple FM–PM transition.

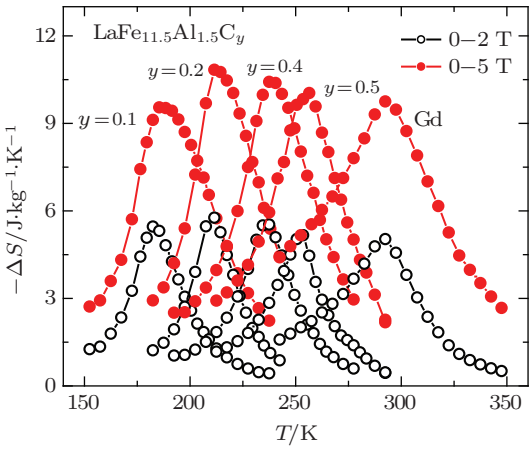


Fig. 8. Temperature dependence of the magnetic entropy change of $LaFe_{11.5}Al_{1.5}C_y$ ($y = 0.1$, 0.2, 0.4, 0.5) compounds compared to that of Gd for magnetic field changes of 0–2 T and 0–5 T, respectively.[34]

For the $LaFe_{13-x}Al_x$ with an FM ground state, the introduction of C significantly enhances both the Curie temperature and the magnetic moment of Fe. The latter causes a growth of the saturation magnetization. For example, as the C content is changed from $y = 0$ to $y = 0.5$, the T_C of $LaFe_{11}Al_2C_y$ increases from 200 K to 291 K, and the Fe magnetic moment shifts from 1.81 μ_B to 1.93 μ_B. A large MCE is observed around the transition temperature for $LaFe_{11}Al_2C_y$, and the peak value of the entropy change is ~ 6.5 J·kg^{-1}·K^{-1} under a field change of 0–5 T. Although the peak of the entropy change is not high, its temperature span is wide (~ 70 K), which gives rise to quite a large refrigeration capacity (RC).[53]

Zhao *et al.*[54] revealed that the introduction of interstitial H atoms can also produce significant effects on magnetic and magnetocaloric properties of $LaFe_{11.5}Al_{1.5}H_y$. The $LaFe_{11.5}Al_{1.5}H_y$ intermetallic with H content between 0.12 and 1.3 displays an FM character, and the Curie temperature increases from ~ 225 K to ~ 295 K as the H concentration changes from $y = 0.12$ to 1.3. The magnetic moment of Fe also shows an increase with the addition of H. It is 1.99 μ_B for $LaFe_{11.5}Al_{1.5}$, and increases to 2.12 μ_B and 2.19 μ_B as y grows to 0.12 and 1.3, respectively. We fit the isothermal magnetization curves to the Inoue–Shimizu model and obtain the Landau coefficients of $\alpha_2(T_C) = 0.118$, -0.063, and -0.373

for $LaFe_{11.5}Al_{1.5}H_x$ ($x = 0.12$, 0.6, 1.3), respectively. This result indicates that the transition nature develops from second-order to first-order with the increasing H concentration. Figure 9(a) presents the temperature-dependent magnetization for $LaFe_{11.5}Al_{1.5}H_x$ under different magnetic fields. The maximal values of ΔS are 5.4 $J{\cdot}kg^{-1}{\cdot}K^{-1}$, 6.2 $J{\cdot}kg^{-1}{\cdot}K^{-1}$, and 6.7 $J{\cdot}kg^{-1}{\cdot}K^{-1}$ under the field change of 0–2 T, and 10.1 $J{\cdot}kg^{-1}{\cdot}K^{-1}$, 11.6 $J{\cdot}kg^{-1}{\cdot}K^{-1}$, and 12.3 $J{\cdot}kg^{-1}{\cdot}K^{-1}$ under 0–5 T, for the compounds with $x = 0.12$, 0.6, and 1.3, respectively. The entropy change increases by 22% as the H concentration increases from 0.12 to 1.3. These results can be ascribed to two effects. One is the strengthening of the first-order nature of the IEM transition as indicated by Landau coefficients $\alpha_2(T)$, which favors enhanced entropy changes. The other is the increase of Fe moment with the introduce of the H atoms, which also enhances the entropy change. However, the interstitial hydrides exhibit low thermal stability. Further studies found that the simultaneous introduction of C and H atoms can remarkably enhance the thermal stability of $LaFe_{13-x}Al_x$ without affecting the excellent magnetic and magnetocaloric properties. For example, $LaFe_{11.5}Al_{1.5}C_{0.2}H_y$ remains stable even when heated to 639 K. As the H content increases from $y = 0$ to 1.0, T_C increases from 212 K to 309 K, and the maximal ΔS increases from 6.7 $J{\cdot}kg^{-1}{\cdot}K^{-1}$ to 8.5 $J{\cdot}kg^{-1}{\cdot}K^{-1}$ for a field change of 0–2 T, and from 11.9 $J{\cdot}kg^{-1}{\cdot}K^{-1}$ to 13.8 $J{\cdot}kg^{-1}{\cdot}K^{-1}$ for 0–5 T

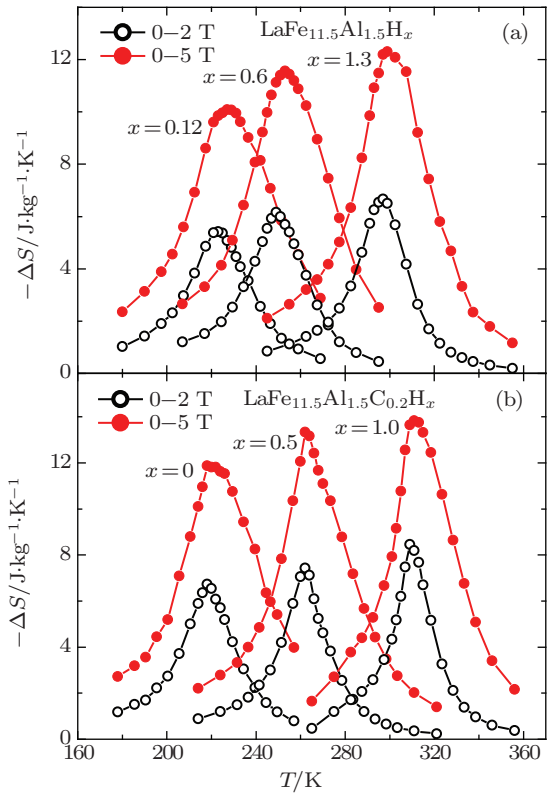


Fig. 9. Temperature dependence of the magnetic entropy change under magnetic field changes of 0–2 T and 0–5 T for (a) $LaFe_{11.5}Al_{1.5}H_x$ ($x = 0.12$, 0.6, 1.3)[54] and (b) $LaFe_{11.5}Al_{1.5}C_{0.2}H_x$ ($x = 0$, 0.5, 1.0).

(Fig. 9(b)). Around room temperature, $LaFe_{11.5}Al_{1.5}C_{0.2}H_{1.0}$ exhibits an entropy change larger than that of Gd by 70% and 42% for the field changes of 0–2 T and 0–5 T, respectively. As is well known, Gd has long been regarded as an excellent refrigerant for magnetic cooling in the room temperature region.

6. Bistable AFM and FM states in $LaFe_{13-x}Al_x$ compounds

Intensive investigations have been carried out for the AFM $LaFe_{13-x}Al_x$ compounds. Wang *et al.*[55] investigated the issues associated with the bistable behavior of AFM and FM states in $LaFe_{13-x}Al_x$ compounds. They chose $LaFe_{11.4}Al_{1.6}$ and constructed a magnetic diagram through measuring temperature/field dependent magnetization (M–T/M–H curves) under different magnetic fields/temperatures. They found that $LaFe_{11.4}Al_{1.6}$ has a Neel temperature at 195 K. Figure 10(a) presents the isothermal magnetization curves of $LaFe_{11.4}Al_{1.6}$ measured at different temperatures. One can notice that at temperatures lower than T_N, an AFM–FM first-order phase transition occurs at a critical field of H_{on} for the field-increasing operation, and a reverse FM–AFM transition takes place at a critical field $H_{off} \ll H_{on}$ for the field-decreasing run. The hysteresis loop around the metamagnetic transition becomes narrow with the increase of temperature and, finally, disappears at T_N. This result evinces the bistable behavior of AFM and FM states with the change of temperature. Based on the field-dependent magnetization measured at different temperatures, a magnetic phase diagram can be constructed in the H–T plane (Fig. 10(b)). The H–T plane is divided into four regions by the H_{on}–T and H_{off}–T curves, corresponding to different magnetic phases. The intermediate section enclosed by the two curves is the AFM region when measured in the field ascending mode and the FM region in the field descending mode. The arrows indicate the direction of the applied magnetic field. To get a thorough understanding of the bistable AFM and FM states and the temperature dependence of the critical field, Wang *et al.* also analyzed the thermal magnetization and the reciprocating thermal magnetization curves measured under different fields, and based on the data thus obtained refined the phase diagram of $LaFe_{11.4}Al_{1.6}$. They found that in the field-increasing case, bistable AFM and FM states appear in the field region of 2 T$< H <$2.2 T and the temperature range of 75 K$< T <$120 K. However, the bistable behavior occurs in wider regions in the field-decreasing case, i.e., 1.7 T $< H <$ 2.2 T, $T <$ 33 K and 45 K$< T <$100 K. Based on the FM–PM transition temperature obtained from the thermal magnetization curves, the boundary between the FM and the PM phases in the H–T plane was determined, as denoted by the dashed line in Fig. 10(b). The triple point of $LaFe_{11.4}Al_{1.6}$ is located at $T = 150$ K, $H = 2.6$ T. The bistable

AFM and FM states in a wide range are closely related to the crystal structure and the magnetic interactions, and to the change of the lattice parameter of $LaFe_{11.4}Al_{1.6}$. This results from the interplay between the elastic energy and the exchange energy. More specifically, the bistable behavior is closely related to the stability of the boundary phase, which is jointly determined by the coupled magnetic interaction and the lattice distortions.

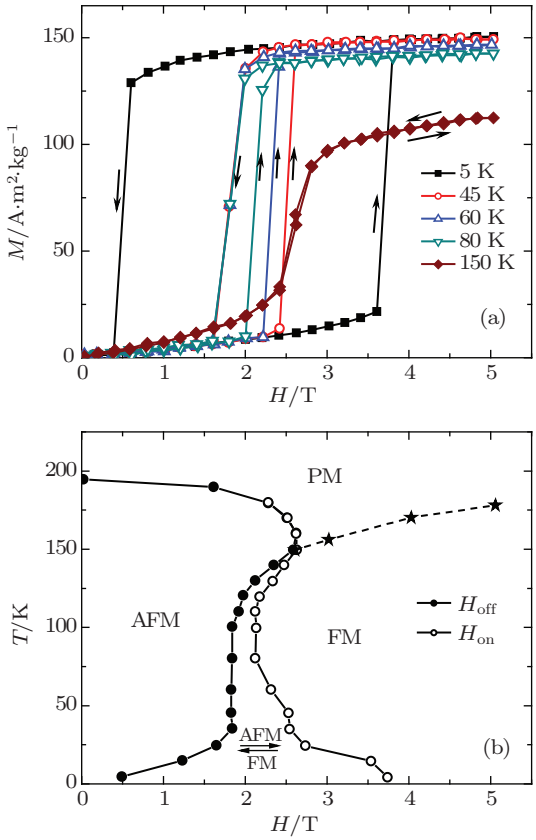


Fig. 10. (a) Isothermal magnetization curves of $LaFe_{11.4}Al_{1.6}$ compound at different temperatures in the field-ascending and field-descending processes. (b) Magnetic phase diagram in H–T for $LaFe_{11.4}Al_{1.6}$ compound.[55]

7. Hyperfine interactions during metamagnetic transition in AFM $LaFe_{11.4}Al_{1.6}$ compound

Wang *et al.*[56] measured the ^{57}Fe Mössbauer spectra of the $LaFe_{11.4}Al_{1.6}$ compound under different applied fields, and investigated the changes of hyperfine parameters during the metamagnetic transition. Figure 11 presents the ^{57}Fe Mössbauer spectra measured at 5 K with different magnetic fields. The relatively broad peaks indicate a wide distribution of the hyperfine fields. Because of the small difference of the hyperfine fields at the Fe_I and Fe_{II} sites, it is difficult to separate the total spectra into sub-spectra of Fe_I and Fe_{II}, and only average hyperfine parameters can be obtained. The specific intensity of the Mössbauer sixline spectra depends on the angle β between the incident γ ray and the effective field. The relatively strong intensity of the second and the fifth peaks in the spectra, $I_{2,5,}$ reveals the rotation direction of the magnetic moment. The $I_{2,5} = 0$ indicates that the hyperfine field is parallel to the external magnetic field. The 2–5 peaks in the spectra of $LaFe_{11.4}Al_{1.6}$, collected at 5 K, gradually disappear with the increasing magnetic field, indicating a gradual rotation of the moment to align with the external field. Figure 12(a) presents intensity $I_{2,5}$ as a function of the external magnetic field.

Figures 12(b) and 12(c) show, respectively, the average hyperfine field $\langle H_{hf} \rangle$ and its rotating angle $\langle \cos\theta \rangle$ as a function of the magnetic field. We can find that the critical field for inducing the metamagnetic transition is about 4 T for $LaFe_{11.4}Al_{1.6}$, consistent with the result from magnetic measurements. If the spatial distribution of Fe's moment is a narrow single peak, $\cos\theta$ actually represents the projection of a unit magnetic moment along the external field. Therefore, figure 12(c) is actually a description of the average rotation of the magnetic moment of Fe with the external magnetic field. Under the impact of the external field, the magnetic moment of Fe rotates continuously towards the field direction. When the applied field exceeds a critical value, the sample exhibits an FM state, and almost all moments are aligned in the field direction. The direction of the magnetic moment varies slightly for further field increases, and a tendency of saturation appears above 8 T. To understand the change of the hyperfine field with the external field, it is necessary to consider the relationship between the hyperfine field and the Fe moment. We know that the hyperfine field can be split up into local and transferred contributions that are directly related to the local moments and the moments of the neighboring atoms, respectively.[57,58] For $LaFe_{11.4}Al_{1.6}$, the local moment changes little with the magnetic field, thus the change of the hyperfine field is mainly caused by the contributions transferred from the neighboring Fe atoms. For the conventional AFM state, due to the symmetric atomic environments around the Fe atoms, the exchange polarization contributions from the neighboring atoms cancel each other, and the transferred contributions disappear. However, in $LaFe_{11.4}Al_{1.6}$, the Fe_{II} site has asymmetric local environments since the substitution of Al for Fe has destroyed the originally symmetric neighboring environments of the Fe_I site. As a result, in the AFM state for $H = 0$, the exchange polarization contributions from the neighboring atoms do not completely cancel each other, and the transferred contributions show up. As shown by our experiments, the transferred contribution is about 6.24 T for the AFM ground state of $LaFe_{11.4}Al_{1.6}$. It increases with the increasing field, and when the external field exceeds a critical value, the magnetic moment approaches a saturation value. In this case, the contribution from the neighboring atoms to the exchange polarization reaches a maximum, thus the transferred contribution does not change any more. The maximal transferred contribution is es-

timated to be 10.66 T.

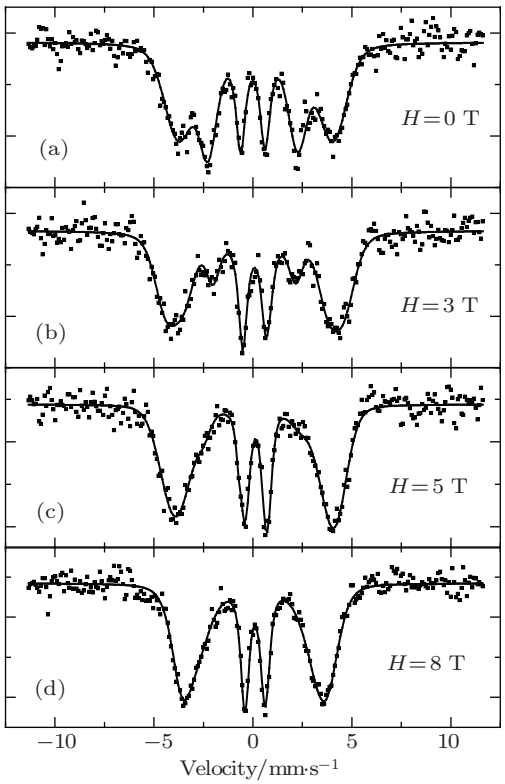


Fig. 11. The ^{57}Fe Mössbauer spectra at 5 K under various applied fields ((a) $H = 0$ T, (b) $H = 3$ T, (c) $H = 5$ T, (d) $H = 8$ T) for $LaFe_{11.4}Al_{1.6}$.[56] The best fit is shown by the solid line.

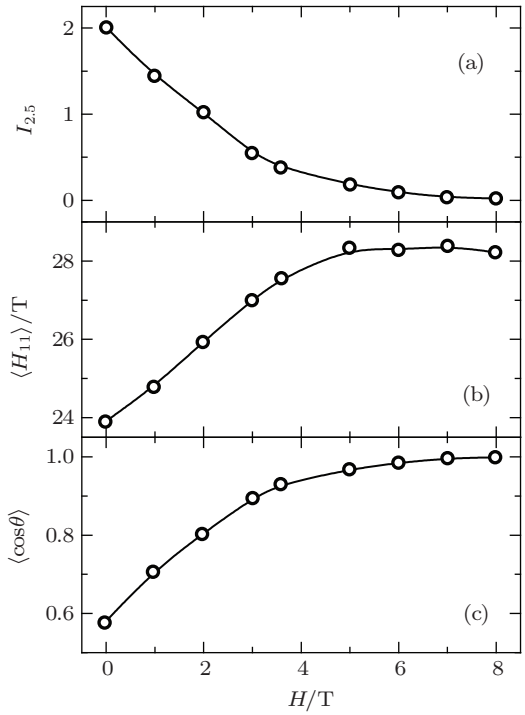


Fig. 12. Applied field dependence of (a) the relative intensity of the second and the fifth lines $I_{2,5}$, (b) the average hyperfine field H_{hf}, and (c) the calculated average $\langle\cos\theta\rangle$ for $LaFe_{11.4}Al_{1.6}$.[56]

Our experimental results indicate that the hyperfine parameters continuously change with the external magnetic field. This result is different from the behavior of first-order transition observed in magnetic measurements. Through calculating the field-dependent change of the average hyperfine field and its rotating angle, it is found that the critical field for the metamagnetic transition is consistent with that derived from the magnetic measurements. The local moment of Fe atoms remains nearly unchanged in the field ascending process, and the local hyperfine field changes little. Thus, the change of the hyperfine field is mainly caused by the transferred contribution due to spin rotation.

8. Summary

(i) With increasing Al content, the $LaFe_{13-x}Al_x$ compounds exhibit AFM ($1.0 \leq x \leq 1.8$), FM ($1.8 < x \leq 4.9$), and mictomagnetic properties ($4.9 \leq x \leq 7.0$) successively. For $LaFe_{13-x}Al_x$ with an AFM ground state, weak AFM properties show up because of the high coordination number around Fe and the short Fe–Fe bond length. An AFM to FM transition can easily be induced by a magnetic field. The AFM–FM transition can also be produced by the substitution of Si for Al, Co for Fe, and magnetic *R* (rare earth atoms) for La, or the introduction of interstitial atoms C and H.

(ii) The coexistence of AFM and FM clusters was observed in compounds $LaFe_{11.4}Al_{1.6-x}Si_x$ ($x = 0.22$), $La_{0.8}Pr_{0.2}Fe_{11.4}Al_{1.6}$, $La_{0.9}Nd_{0.1}Fe_{11.5}Al_{1.5}$, and $LaFe_{11.4}Al_{1.6}C_{0.02}$. Over a considerably wide temperature range below the Neel temperature, field-induced AFM–FM and FM–AFM transitions take place. Meanwhile, an obvious relaxation behavior was observed around the transition temperature. With the increase of the magnetic field, the ratio of the FM phase grows, and the compounds completely transform into the FM state under high magnetic fields.

(iii) For compounds $La_{1-x}R_xFe_{11.5}Al_{1.5}$ (*R*=Ce, Pr, Nd), the content of *R* generally cannot exceed 30% while retaining a stable $NaZn_{13}$ structure. It becomes easier for magnetic field to induce an AFM–FM transition in the presence of *R*, and the threshold field for the AFM–FM transition decreases considerably with the increase of the *R* content. The effect of *R* on the magnetic properties of the compounds increases progressively along the sequence of Ce, Pr, and Nd.

(iv) Through measuring temperature/field dependent magnetization under different fields/temperatures for $LaFe_{11.4}Al_{1.6}$, a magnetic diagram was constructed and bistable AFM and FM states were observed. Near the critical region in the diagram, the bistable behavior is different for field increasing and decreasing. In the field-increasing case, the bistable AFM and FM states appear at the field region about 2 T$< H <$ 2.2 T and the temperature region about 75 K$< T <$120 K. But for the field-decreasing

case, the bistable behavior occurs in wider regions, i.e. 1.7 T$< H <$ 2.2 T, $T <$ 33 K and 45 K$< T <$100 K.

(v) The hyperfine parameters display continuous changes with the external magnetic field for $LaFe_{11.4}Al_{1.6}$. This phenomenon may be related to the fact that the intrinsic moments in the FM and the AFM states are nearly the same. Considering the fact that the local moment of Fe atoms remains nearly unchanged upon the application of magnetic field and the local hyperfine field changes little, we believe that the change of the hyperfine field is mainly caused by the transferred contribution due to spin rotation.

(vi) The Curie temperature of the $LaFe_{13-x}Al_x$-based compounds can be promoted to room temperature by introducing Co or interstitial atoms C and H, and a large MCE was observed around the transition temperature. The room temperature entropy changes of $LaFe_{10.88}Co_{0.95}Al_{1.17}$ are 4.5 J·kg^{-1}·K^{-1} and 9.0 J·kg^{-1}·K^{-1} for the field changes of 0–2 T and 0–5 T, respectively. Simitanously introducing C and H enhances the thermal stability of the compounds. For example, $LaFe_{11.5}Al_{1.5}C_{0.2}H_y$ shows not only an excellent thermal stability around room temperature but also a large entropy change. The entropy changes are 8.5 J·kg^{-1}·K^{-1} and 13.8 J·kg^{-1}·K^{-1} for 0–2 T and 0–5 T, respectively, exceeding that of Gd (5.0 J·kg^{-1}·K^{-1} and 9.7 J·kg^{-1}·K^{-1}). It therefore is a potential candidate for magnetic refrigerants.

References

[1] Warburg E 1881 *Ann. Phys.* **13** 141
[2] Brown G V 1976 *J. Appl. Phys.* **47** 3673
[3] Lee J S 2004 *Phys. Stat. Sol.* (b) **241** 1765
[4] Pecharsky V K and Gschneidner Jr K A 1997 *Phys. Rev. Lett.* **78** 4494
[5] Guo Z B, Du Y W, Zhu J S, Huang H, Ding W P and Feng D 1997 *Phys. Rev. Lett.* **78** 1142
[6] Hu F X, Shen B G and Sun J R 2000 *Appl. Phys. Lett.* **76** 3460
[7] Hu F X, ShenB G, Sun J R and Wu G H 2001 *Phys. Rev.* B **64** 132412
[8] Wada H and Tanabe Y 2001 *Appl. Phys. Lett.* **79** 3302
[9] Tegus O, Bruck E, Buschow K H J and de Boer F R 2002 *Nature* **415** 150
[10] Hu F X, Shen B G, Sun J R and Zhang X X 2000 *Chin. Phys.* **9** 550
[11] Hu F X, Shen B G, Sun J R, Cheng Z H, Rao G H and Zhang X X 2001 *Appl. Phys. Lett.* **78** 3675
[12] Zhang H W, Wang F, Zhao T Y, Zhang S Y, Sun J R and Shen B G 2004 *Phys. Rev.* B **70** 212402
[13] Wang F W, Wang G J, Hu F X, Kurbakov A, Shen B G and Cheng Z H 2003 *J. Phys.: Condens. Matter* **15** 5269
[14] Di N L, Cheng Z H, Li Q A, Wang G J, Kou Z Q, Ma X, Luo Z, Hu F X and Shen B G 2004 *Phys. Rev.* B **69** 224411
[15] Wang G J, Wang F, Di N L, Shen B G and Cheng Z H 2006 *J. Magn. Magn. Mater.* **303** 84
[16] Shen B G, Sun J R, Hu F X, Zhang H W and Cheng Z H 2009 *Adv. Mater.* **21** 4545
[17] Hu F X, Shen B G, Sun J R, Wang G J and Cheng Z H 2002 *Appl. Phy. Lett.* **80** 826
[18] Chen Y F, Wang F, Shen B G, Hu F X, Cheng Z H, Wang G J and Sun J R 2002 *Chin. Phys.* **11** 741
[19] Chen Y F, Wang F, Shen B G, Hu F X, Sun J R, Wang G J and Cheng Z H 2003 *J. Phys.: Condens. Matter* **15** L161
[20] Wang F, Chen Y F, Wang G J, Sun J R and Shen B G 2003 *Chin. Phys.* **12** 911
[21] Chen Y F, Wang F, Shen B G, Hu F X, Sun J R, Wang G J and Cheng Z H 2003 *J. Appl. Phys.* **93** 1323
[22] Zhao J L, Shen J, Hu F X, Li Y X, Sun J R and Shen B G 2010 *J. Appl. Phys.* **107** 113911
[23] Shen J and Zhao J L 2012 *J. Appl. Phys.* **111** 07A908
[24] Zhao J L, Shen J, Zhang H, Xu Z Y, Wu J F, Hu F X, Sun J R and Shen B G 2012 *J. Alloys Compd.* **520** 277
[25] Palstra T T M, Nieuwenhuys G J, Mydosh J A and Buschow K H J 1984 *J. Appl. Phys.* **55** 2367
[26] Helmholdt R B, Palstra T T M, Nieuwenhuys G J, Mydosh J A, van der Kraan A M and Buschow K H J 1986 *Phys. Rev.* B **34** 169
[27] Palstra T T M, Nieuwenhuys G J, Mydosh J A and Buschow K H J 1985 *Phys. Rev.* B **31** 4622
[28] Palstra T T M, Werij H G C, Nieuwenhuys G J, Mydosh J A, de Boer F R and Buschow K H J 1984 *J. Phys.* F: *Met. Phys.* **14** 1961
[29] Shcherbakova Ye V, Korolyov A V and Podgornykh S M 2001 *J. Magn. Magn. Mater.* **237** 147
[30] Hu F X, Shen B G, Sun J R, Cheng Z H and Zhang X X 2000 *J. Phys.: Condens. Matter* **12** L691
[31] Hu F X, Shen B G, Sun J R and Cheng Z H 2001 *Phys. Rev.* B **64** 012409
[32] Irisawa K, Fujita A, Fukamichi K, Yamazaki Y, Iijima Y and Matsubara E 2001 *J. Alloy Compd.* **316** 70
[33] Hu F X, Wang G J, Wang J, Sun Z G, Dong C, Chen H, Zhang X X, Sun J R, Cheng Z H and Shen B G 2002 *J. Appl. Phys.* **91** 7836
[34] Wang F, Chen Y F, Wang G J, Sun J R and Shen B G 2004 *J. Phys.: Condens. Matter* **16** 2103
[35] Liu X B, Altounian Z and Ryan D H 2004 *J. Phys.* D: *Appl. Phys.* **37** 2469
[36] Irisawa K, Fujita A, Fukamichi K, Yamada M, Mitamura H, Goto T and Koyama K 2004 *Phys. Rev.* B **70** 214405
[37] Liu G J, Sun J R, Zhao T Y and Shen B G 2006 *Solid State Commun.* **140** 45
[38] Zhang H W, Chen J, Liu G J, Zhang L G, Sun J R and Shen B G 2006 *Phys. Rev.* B **74** 212408
[39] Chen J, Zhang H W, Zhang L G, Sun J R and Shen B G 2007 *J. Appl. Phys.* **102** 113905
[40] Wang F, Wang G J, Sun J R and Shen B G 2008 *Chin. Phys.* B **17** 3087
[41] Hu F X, Shen B G, Sun J R, Pakhomov A B, Wong C Y, Zhang X X, Zhang S Y, Wang G J and Cheng Z H 2001 *IEEE Transactions on Magnetics* **37** 2328
[42] Wang G J, Hu F X, Wang F and Shen B G 2004 *Chin. Phys.* **13** 546
[43] Wang F, Zhang J, Chen Y F, Wang G J, Sun J R and Shen B G 2004 *Phys. Rev.* B **69** 094424
[44] Dong Q Y, Zhang H W, Sun J R and Shen B G 2008 *J. Phys.: Condens. Matter* **20** 135205
[45] Liu G J, Sun J R, Shen J, Gao B, Zhang H W, Hu F X and Shen B G 2007 *Appl. Phys. Lett.* **90** 032507
[46] Zou J D, Shen B G, Gao B, Shen J and Sun J R 2009 *Adv. Mater.* **21** 693
[47] Shen J, Li Y X, Gao B, Sun J R and Shen B G 2007 *J. Magn. Magn. Mater.* **310** 2823
[48] Wang F 2005 *Magnetic and Magnetocaloric Properties in* $NaZn_{13}$*-type* La(Fe, *M*)$_{13}$ *Compounds* (PhD thesis) (Beijing: Institute of Physics, Chinese Academy of Sciences) (in Chinese)
[49] Dong Q Y, Chen J, Zhang H W, Sun J R and Shen B G 2008 *J. Phys.: Condens. Matter* **20** 275235
[50] Perez-Reche F J, Stipcich M, Vives E, Manosa L, Planes A and Morin M 2004 *Phys. Rev.* B **69** 064101
[51] Chen J, Zhang H W, Zhang L G, Dong Q Y and Wang R W 2006 *Chin. Phys.* **15** 0845
[52] Chen J, Dong Q Y, Zhang H W, Zhang L G, Sun J R and Shen B G 2009 *J. Magn. Magn. Mater.* **321** 3217
[53] Wang F, Chen Y E, Wang G J, Sun J R and Shen B G 2004 *Chin. Phys.* B **13** 393
[54] Zhao J L, Shen J, Shen B G, Hu F X and Sun J R 2010 *Solid State Commun.* **150** 2329
[55] Wang G J, Wang F and Shen B G 2005 *Acta Phys. Sin.* **54** 1410 (in Chinese)
[56] Wang G J 2004 *Magnetic Properties, Hyperfine Interactions, and Physics of Magnetic Entropy Change in* La(Fe, *M*)$_{13}$ *Compounds* (PhD thesis) (Beijing: Institute of Physics, Chinese Academy of Sciences) (in Chinese)
[57] Stearns M B 1971 *Phys. Rev.* B **4** 4081
[58] Blügel S, Akai H, Zeller R and Dederichs P H 1987 *Phys. Rev.* B **35** 3271